Available online at www.sciencedirect.com
SCIENCE DIRECT
Journal of Molecular Graphics and Modelling 24 (2005) 94–101
Journal of Molecular Graphics and Modelling
www.elsevier.com/locate/JMGM

Assessment of a mechanism for reactive inhibition of carboxypeptidase A with QM/MM methods

Lily Phoon, Neil A. Burton *

School of Chemistry, University of Manchester, Manchester M13 9PL, UK

Accepted 30 June 2005
Available online 6 September 2005

Abstract

The mechanism for inhibition of carboxypeptidase A (CPA) by the two enantiomers of a reactive inhibitor, *N*-(2-chloroethyl)-*N*-methylphenylalanine, has been investigated using computational methods. Quantum mechanical and molecular mechanical (QM/MM) methods have been employed to find likely enzyme binding conformations by comparison with the observed rates of inactivation of the enzyme. The study has shown that the enzyme active site appears to be flexible enough to allow the nucleophilic deactivation reactions of both the (*R*) and (*S*) forms of a model of the inhibitor to be catalysed by the Zn(II) cofactor of CPA.

Keywords: *N*-(2-Chloroethyl)-*N*-methylphenylalanine; QM/MM; Carboxypeptidase A; Enzyme inhibition; Enantiomer binding; Reactive inhibition; Density functional theory

1. Introduction

Metalloproteinases, particularly those containing Zn, are important targets for a wide range of clinical conditions and carboxypeptidase A (CPA) has been a major target for a wide range of inhibitors and mechanistic studies [1,2]. A large number of inhibitors are known for CPA but by far the most common are substrate/transition state analogues or Zn-chelators [3] which act via a competitive inhibition mechanism. Computational prediction of the activity of such inhibitors is often through the study of their relative binding free energies, which can be readily obtained using a variety of docking approaches [4,5] using either empirical scoring functions or classical force-fields [6]. In this paper, we shall consider the action of an alternative novel suicide inhibitor, *N*-(2-chloroethyl)-*N*-methylphenylalanine (CEMPA, Fig. 1), which was introduced by Park et al. [7]; and we shall highlight how quantum mechanical and molecular mechanical (QM/MM) methods may be used when inhibition involves a reactive mechanism.

Although competing mechanisms for CPA catalysis with various substrates have been proposed from both experimental and computational studies [8–11] it is now widely accepted that CPA cleaves the C-terminal amino acid residue of a natural peptide substrate, e.g. glycyl-L-tyrosine (GLT), via a general acid–base mechanism involving an activated water molecule. This mechanism is facilitated by a Zn(II) ion which is coordinated into the active site by His-69, Glu-72 and His-196. Arg-145 binds the terminal carboxylate of the substrate, aligning it for nucleophilic attack; and the primary recognition pocket, S_1', is hydrophobic to bind the phenyl side chain of the substrate. Perhaps the most controversial aspect of the mechanism is the specific nature of the nucleophile: Christianson and Lipscomb [12] proposed that a Zn-bound water molecule is activated, in part by Glu-270, to generate a more powerful hydroxyl nucleophile. A schematic showing the active site corresponding to this mechanism is shown in Fig. 2. Alternatively, Mock has proposed [13] for certain substrates that the Zn ion could directly stabilise the developing oxyanion of the substrate following nucleophilic attack by a water molecule which may be activated to hydroxyl by the substrate itself.

* Corresponding author. Tel.: +44 161 275 4684; fax: +44 161 275 4734.
E-mail address: neil.burton@manchester.ac.uk (N.A. Burton).

1093-3263/$ – see front matter © 2005 Elsevier Inc. All rights reserved.
doi:10.1016/j.jmgm.2005.06.004

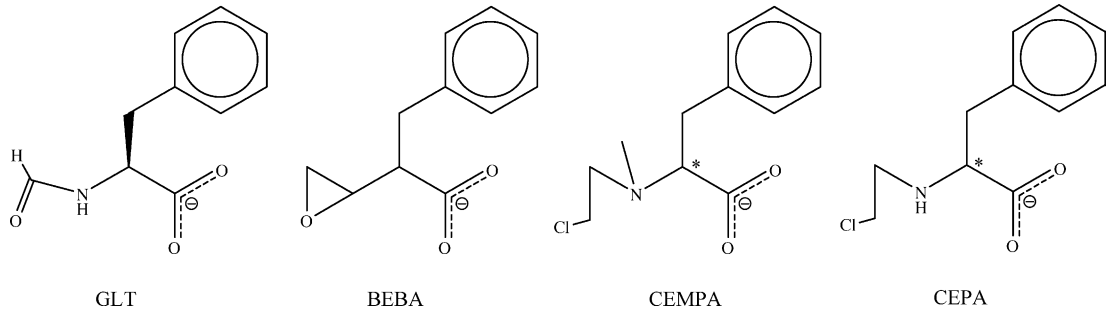

Fig. 1. Structures of natural substrate (GLT), inhibitors (BEBA and CEMPA) and model inhibitor (CEPA).

Although we do not address this mechanistic debate in this work, we note that in the case of the CEMPA inhibition reaction, considered here, an alternative pathway is likely to operate which implicates Glu-270 as the nucleophile and the Zn(II) ion to be directly involved in stabilising the intermediate (or transition state). Other residues, such as Arg-145 and the S_1' recognition site remain important to recognise the inhibitor which is based on the same template as GLT (Fig. 1). This mechanism was the basis on which the CEMPA inhibitor was designed [7] following earlier studies [14] using 2-benzyl-3,4-epoxy-butanoic acid (BEBA, Fig. 1): the oxirane ring of BEBA was shown by structural studies to undergo a ring cleavage reaction initiated by the nucleophilic attack of the carboxylate of Glu-270 resulting in an inactive, covalently bound, final state.

With CEMPA, deactivation is believed to similarly occur with Glu-270 as the nucleophile (Fig. 3) to form a covalent linkage to the inhibitor (**3**), possibly via an aziridinium ion intermediate (**2**). The first step in this reaction sequence (Fig. 3: step (a)), to displace the chloride ion, is likely to be the rate-limiting step. Interestingly, the (*R*) enantiomer of CEMPA, which mimics the natural L-amino acid substrate, was found to be more effective as a CPA inactivator than the alternative (*S*)-enantiomeric form [7]. This was attributed to the likelihood that the (*R*)-form of CEMPA would be bound with its chloro-group directly coordinated to the Zn(II), as found by analogy with the crystal structures of the GLT natural substrate and other Zn-chelating inhibitors, whereas if the phenyl and carboxylate groups were properly bound in the (*S*)-form, the chloro-group would find difficulty in binding in close proximity to Zn. Thus, aziridinium ion formation (or transition state formation) for the (*S*)-form would be relatively slower than for the (*R*)-form in which the Zn ion could actively stabilise the forming transition state. In this paper, we shall propose that the experimentally observed relative rates of the (*R*)- and (*S*)-forms are sufficiently similar that Zn-stabilisation would be necessary for both enantiomers, and that the flexibility of CPA could allow both (*R*)- and (*S*)-forms to bind the chloro-group within the coordination sphere of the Zn.

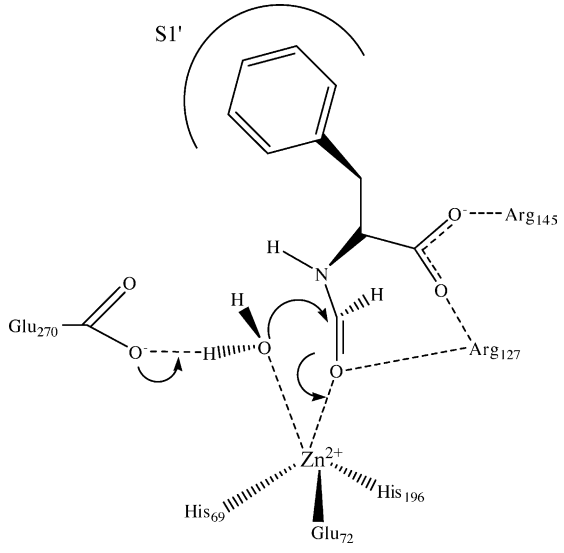

Fig. 2. Active site of CPA with GLT substrate.

Computational approaches utilising classical force-fields or empirical free-energy functions may be inappropriate for the study of inhibition when the key inactivation step involves the breaking or forming of covalent bonds; in such cases, quantum mechanical (QM) potentials should be used. Although significant advances have been made enabling relatively large systems to be studied with QM methods, their routine use for binding and inhibition is often prohibitively uneconomic. In this study we have used a quantum mechanical and molecular mechanical method [15,16] which will treat the smaller reactive part of the system, the QM region, with a QM potential which includes terms to describe the electrostatic and steric constraints due to the rest of the system: the enzyme environment. These methods have grown in popularity in recent years and have been particularly successful for the study of enzyme catalysis [17,18] and condensed phase reactivity.

In this paper we shall first consider the inhibition mechanism in the absence of the protein using simple models for the substrate and the active site. Finally, more realistic models will be studied using the QM/MM method to include more of the enzyme environment and to compare the rate limiting step of the deactivation mechanism for two enantiomeric forms of CEMPA; in these, we shall compare our activation barriers with the experimental kinetic observations as a guide to assess the validity of the binding model and mechanism.

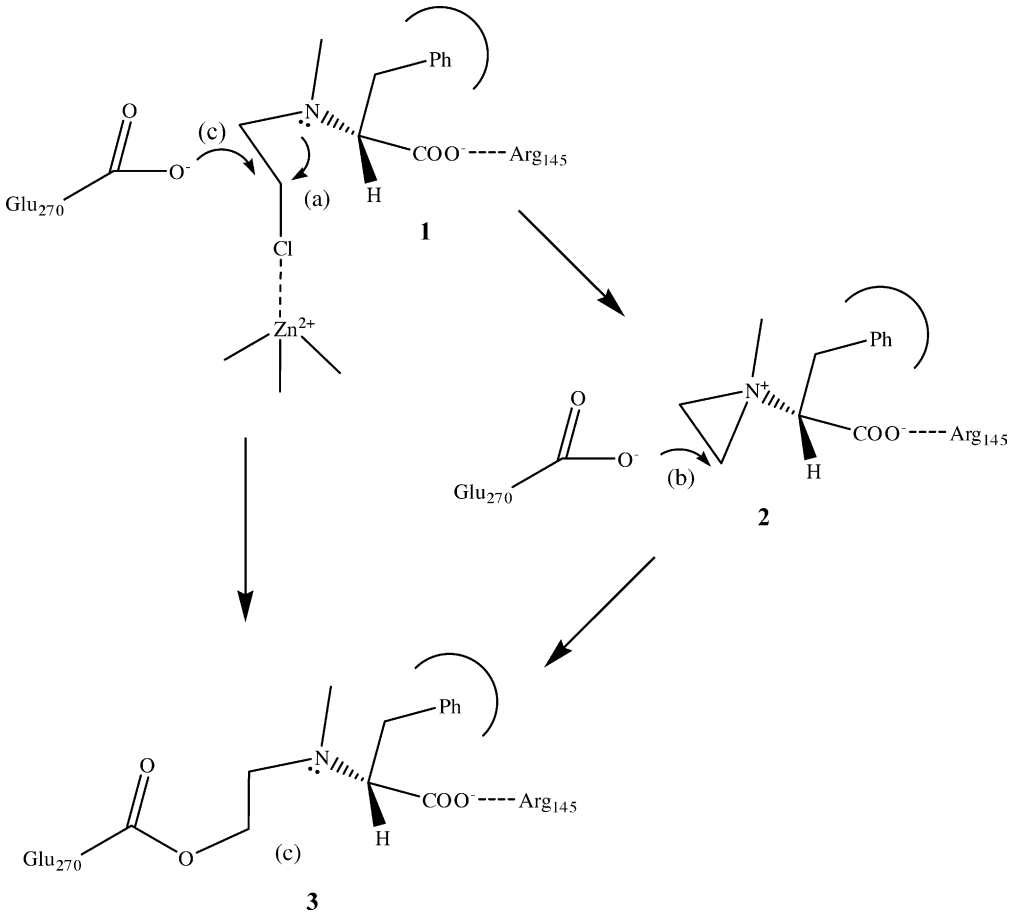

Fig. 3. (a) Formation of an aziridinium intermediate from CEMPA; (b) inactivation of the aziridinium intermediate by Glu-270; and (c) direct inactivation of CEMPA by Glu-270.

2. Computational details

In order to assess the stabilisation effect of a Zn ion on the transition state (TS) during the inactivation process (assuming the formation of an aziridinium intermediate from the CPA substrate, step (a) in Fig. 3), geometry optimisations of the substrate and TS structures were performed both in the presence of a model for the Zn(II) cofactor, and also in its absence. Density functional theory (DFT) methods were used using the 6-31G(d) basis set and the B3LYP exchange-correlation functional [19]. A simple model, $[Zn(NH_3)_2(HCO_2)]^+$ was chosen to mimic the cofactor, Zn(His-69)(His-196)(Glu-72).

The relative energies of various models of the CEMPA substrate, in both (*R*)- or (*S*)-enantiomeric forms, and their corresponding transition states, were also obtained using hybrid QM/MM calculations in the full inhibitor bound protein system using a modified version of the Gaussian program [19]. The enzyme, which was treated using the Cornell et al. [20] standard force-field for AMBER, was also subjected to both molecular dynamics simulation and minimisation to obtain several representative configurations to be used in QM/MM calculations: for each enzyme configuration chosen, the atoms treated at the molecular mechanical level (MM region) were fixed during the QM/MM optimisation procedure. For the inhibitors and substrates, standard MM parameters were selected and new electrostatic potential derived (ESP) charges were computed at the Hartree–Fock level with the 6-31G(d) basis set.

The QM region, shown in Fig. 4, included the substrate, Zn atom and the side chains of His-69, His-196, Glu-72, Glu-270 and Arg-145. The link-atom method was used where partitioning necessitated the disruption of a covalent bond between the QM and MM regions (shown in Fig. 4); all amino acids were terminated with hydrogen link atoms at the C_α positions and the benzyl group of the substrate was not included in the QM region. In each case, the positions of the atoms in the QM region were optimised at the AM1 semi-empirical level and single point energies were obtained, at the B3LYP/6-31G(d) level, at the respective AM1 stationary point. We have found in previous studies [21] that these methods can be quite reliable and useful where the aim is to distinguish inhibition mechanisms when the active sites are relatively large and a number of conformations of the enzyme environment need to be investigated. To simplify the QM/MM and binding calculations, *N*-(2-chloroethyl)-phe-

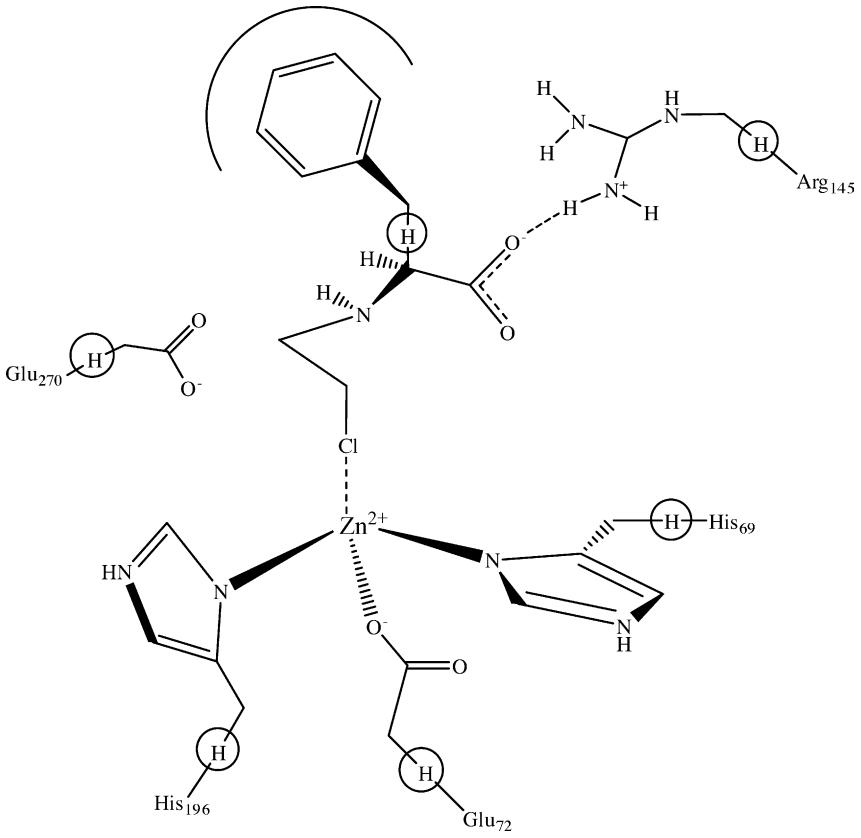

Fig. 4. QM region used in the CPA/CEPA substrate and transition state QM/MM calculations. Link atoms are circled.

nylalanine (CEPA) was used as a model for the CEMPA inhibitor, replacing the (*N*)-methyl group with H. Although we would anticipate some steric effects from this substitution, by analogy with the binding of GLT, which also has this substitution, we assume the differences to be relatively minor.

An initial enzyme structure was created based upon the X-ray coordinates of CPA from *Bos taurus* (3CPA) resolved to 2 Å [12]. The structure, including the GLT substrate, was protonated, solvated with 5591 TIP3P water molecules and heated to 300 K over 150 ps of molecular dynamics simulation using the AMBER program [22]. We shall denote this initial structure as CPA + GLT. GLT was then removed from this structure and several enzyme configurations were generated with either the (*R*)- or the (*S*)-form of the CEPA bound.

3. Assessment of the CPA structure and QM/MM calculations with GLT

The initial CPA + GLT structure was assessed by performing a QM/MM study of the rate limiting reaction of the GLT substrate with a single water molecule coordinated to the Zn ion. The same QM/MM protocol, described earlier for the inhibitor studies, was followed using the AM1 hamiltonian; in this case a QM active site which not only included the imidazole groups of His-69 and His-196, and the carboxylate side chains of Glu-72 and Glu-270, but also the catalytic water, and the full GLT substrate. A transition state corresponding to nucleophilic attack at the carbonyl of GLT by hydroxyl, with the water proton mostly dissociated onto Glu-270, was found and compared with the corresponding step in the AM1 study by Alvarez-Santos; in our case the activation barrier of 33 kcal mol^{-1} is in fair agreement with the previously published barriers, 28 kcal mol^{-1} [8] and 24 kcal mol^{-1} [9], considering that the QM region used here was smaller than the QM gas phase models used in the previous studies.

4. Formation of the aziridinium intermediate using model system

In this section we shall investigate simple gas phase models to mimic the formation of the aziridinium intermediate. In the absence of any amino acid residues representative of the enzyme environment, gas phase models will not be able to distinguish between the (*R*)- and (*S*)-stereoisomers; however, they can be used to approximate the effect of specific enzyme features, such as the Zn cofactor,

on the mechanism. We shall use two gas phase models: the first will be based on chloroethylamine to model the CEMPA molecule in the absence of other residues or a coordinating zinc ion; and the second will include a Zn^{2+} complex to stabilise the leaving chloride ion during the intramolecular nucleophilic reaction of CEMPA. The stationary point structures for the CEMPA model (labelled R1) and its corresponding transition state (TS1) are shown in Fig. 5(a) at the B3LYP/6-31G(d) level as described earlier. The stationary point structures for the larger system, including the model for the Zn cofactor (R2 and TS2), are shown in Fig. 5(b). The potential energy reaction barriers for the two cases, each computed as the difference between the respective TS and reactant energies, were found to be 45.9 kcal mol^{-1} and 6.4 kcal mol^{-1} for the substrate only and with the Zn models, respectively. The relative difference between these barriers is over 30 kcal mol^{-1}; as we shall see, this energy difference is somewhat larger than that predicted between the (*R*)- and (*S*)-isomers in CPA experimentally.

In their assessment of the CEMPA inhibition process, Park et al. [7] observed first order rate constants for the inactivation of CPA activity. Assuming the same experimental conditions for the (*R*)- and (*S*)-forms, we can estimate the relative difference in activation barriers using transition state theory; the resulting energy difference, based upon $k_{obs}/[I]_0$ values of 1.26 M^{-1} s^{-1} and 0.86 M^{-1} s^{-1} for the (*R*)- and (*S*)-forms, respectively, would be 0.2 kcal mol^{-1}. We should emphasise that our computational methods cannot achieve a level of accuracy able to reliably predict such a small differential effect. Since the gas phase energy differences, between inhibition with and without coordination to the Zn cofactor, are likely to be considerably greater than the computational errors of the methodology used, our approach to understand the inhibition mechanism will be to find binding conformations for which the

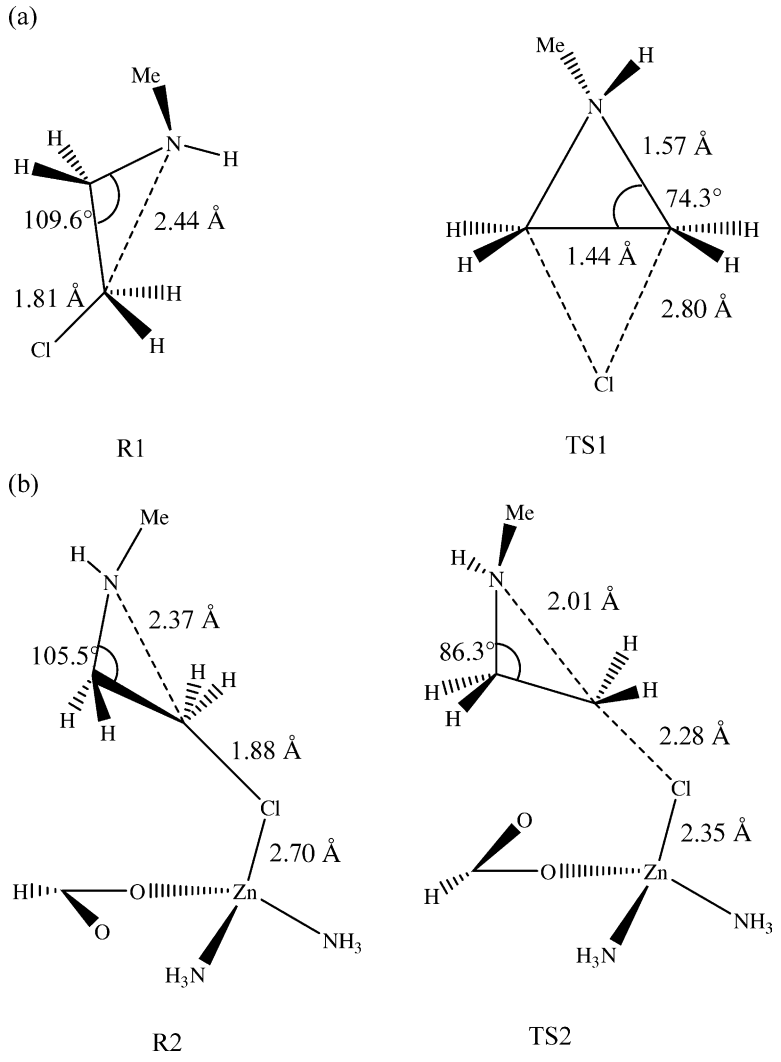

Fig. 5. Gas phase reactant model and transition state stationary points for aziridinium intermediate formation at the B3LYP/6-31G(d) level (a) without Zn^{2+} present (R1 and TS1) and (b) with the Zn^{2+} cofactor model present (R2 and TS2).

activation energy difference between the (*R*)- and (*S*)-forms becomes negligible. We may then have some confidence that the binding conformations are representative of those experienced experimentally.

5. Protein conformations and selectivity

We may now turn to the first enzyme configurations to be assessed: these were based upon two structures which were created by docking the initial GLT based CPA structure with the (*R*)- and (*S*)-forms of CEPA, respectively, using the Autodock program [23]. Unfortunately the docking approach, although allowing substrate flexibility, rarely gave low-energy structures with the chloro-group coordinated to zinc for either enantiomer, preferring instead to coordinate the carboxylate of CEPA to Zn. Consequently higher energy structures with the chloro-group of CEPA bound within the coordination sphere of the Zinc ion were chosen for further study; however, the structure found for the (*S*)-form was rather strained and it was subsequently not possible to find a transition state en route to the aziridinium intermediate due to the steric constraints imposed by the active site residues in this configuration. The greater difficulty of binding the (*S*)-form so that the chloro-group can be coordinated to the Zn ion would correlate with the observed inhibition constants, K_i, observed by Park et al. [7] They observed that K_i was 0.36 μM and 2.5 μM, respectively, for the (*R*)- and (*S*)-forms.

QM/MM stationary points were found for an initial docked (*R*)-structure and the transition state for aziridinium intermediate formation, and an initial reaction barrier was obtained. The Zn–Cl distances for the reactant and transition states are 2.23 Å and 2.18 Å, respectively. At the AM1 level, the barrier was found to be 42.8 kcal mol^{-1} which was significantly reduced to 11.7 kcal mol^{-1} at the B3LYP/6-31G(d) DFT level. It is important to note that the DFT barriers are approximations to the barrier since they are dependent upon the stationary points obtained for the AM1 potential energy surface. A potential energy barrier of between 10 kcal mol^{-1} and 15 kcal mol^{-1} would appear to be quite realistic giving us confidence that such a bound (*R*)-CEMPA structure could indeed lead to reaction and inactivate the enzyme. To indicate the sensitivity in the binding, it is interesting to compare the barriers with a larger QM/MM calculation where the (*R*)-CEPA substrate with phenyl group is included in the QM region. In this case the reactant structure, when re-optimised, was strained as shown by a Zn–Cl distance >3 Å and a lower barrier, 8.3 kcal mol^{-1} at the DFT level, since the enzyme structure is still quite optimal for the transition state, again with a Zn–Cl distance of 2.18 Å.

Since we were unable to find a transition state for the (*S*)-form in the docked structure, a further 150 ps of MD simulation was performed around the docked inhibitor with its internal coordinates frozen. A transition state was found for the resulting enzyme structure with an activation barrier of 29.3 kcal mol^{-1} at the DFT level; the large difference in the activation energies of the (*R*)- and (*S*)-forms at this stage does not correlate with the experimental data.

This case highlights one of the main difficulties associated with traditional computational docking or virtual screening methods: their success is known to be highly dependent upon the target structure used. It is well known that the active sites of many proteins are flexible, and although ligand flexibility has been efficiently incorporated into docking techniques by allowing some torsional variations, docking approaches incorporating protein flexibility are not as well established. To address this issue in this study, we have followed a common approach which is to bind into a range of protein conformations.

6. Relaxation of the enzyme structure

One of the main rationales of this work is to determine whether QM/MM methods can be used to assess which protein configurations are likely to be important for binding by correlating computed reactivity data, which will be extremely sensitive to these structures, with experimental observations. To establish this principle, we shall now consider several alternative protein configurations. Since we are specifically looking for conformations which can accommodate the stereo-specific forms of CEMPA, the protein structures chosen were generated to favour binding in each case.

In order to allow some relaxation of the enzyme structure within the QM/MM framework, the respective enzyme structures for the (*R*)- and (*S*)-forms were then further minimised at the MM level around the QM/MM inhibitor bound structures. The activation barriers with the resulting structures, labelled CPA-min, and which correspond to new reactant and transition states optimised at the QM/MM level, are shown in Table 1. Although these barriers are still high, at 22 kcal mol^{-1} and 18 kcal mol^{-1} for (*R*) and (*S*), respectively, it is clear that the Zn cofactor is now participating in both reactions. Closer inspection of these stationary points shows that the (*R*)-reactant form has probably been destabilised relative to the other structures.

Table 1
Summary of the potential energy reaction barriers, $\Delta E^{\ddagger}$ (kcal mol^{-1}) using the various models at the B3LYP/6-31G(d) level

	$\Delta E^{\ddagger}$ (*R*)-CEPA	$\Delta E^{\ddagger}$ (*S*)-CEPA	$\Delta\Delta E^{\ddagger}$ (*R*) → (*S*)
Gas phase	6.4	45.9	39.5
CPA-GLT[a]	11.7	29.3[b]	17.6
CPA-min[a]	21.5	18.2	−3.3
CPA-MD[a]	13.2	13.2	0.0
Experiment	–	–	0.2

[a] QM/MM at the B3LYP/6-31G(d)//AM1 level.
[b] Enzyme structure was relaxed to obtain a transition state for (*S*)-CEPA (see text).

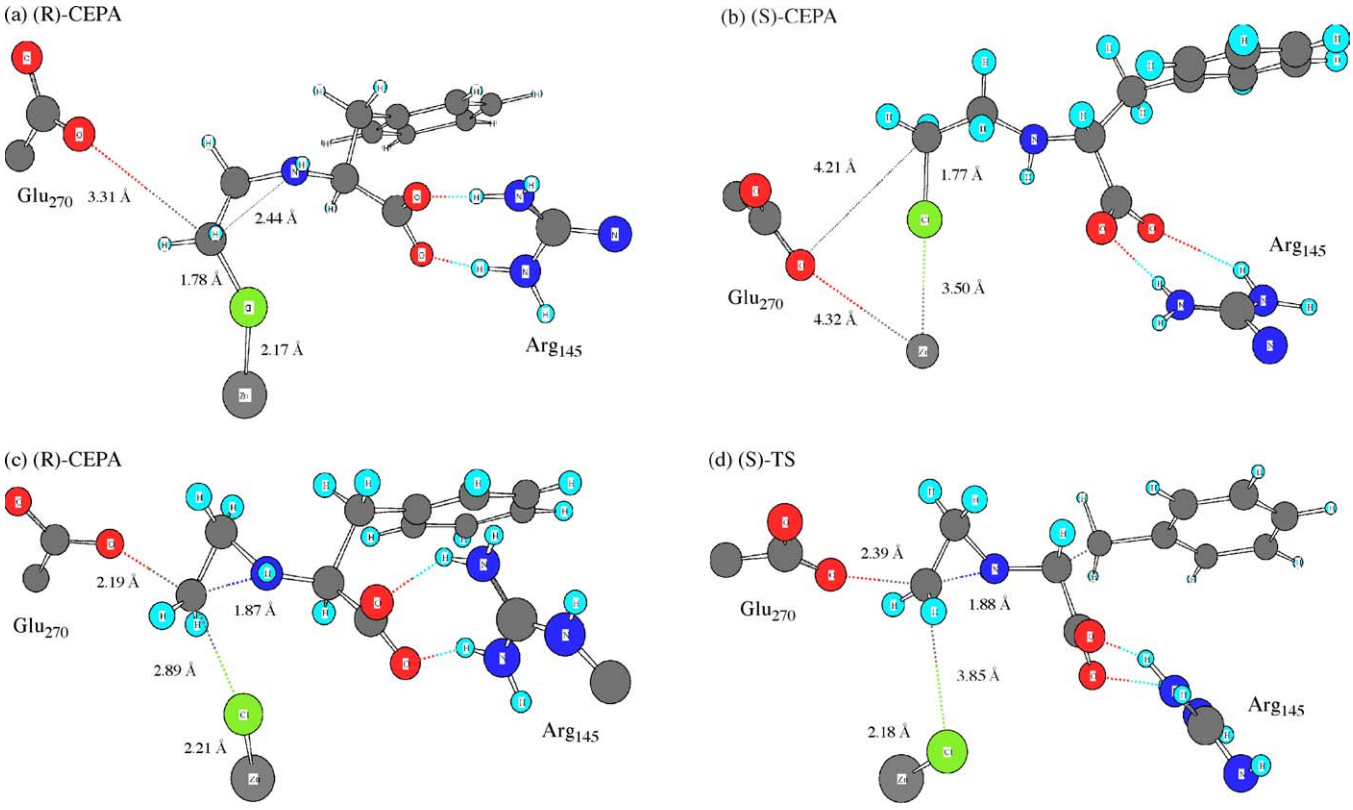

Fig. 6. Final optimised QM/MM structures of (a) (*R*)-CEPA; (b) (*S*)-CEPA and (c) (*R*)-TS and (d) (*S*)-TS.

To obtain further structures, 150 ps of MD was performed at 300 K starting from the CPA-min reactant structures, again fixing the internal coordinates of the inhibitor in each case. It was anticipated that these conformations would be less optimal and thus allow less sterically constrained transition states. Indeed, when the transition states were found (Fig. 6: *R*-TS and *S*-TS, respectively), the energy barriers were lower and almost identical for the (*R*)- and (*S*)-forms: 13.2 kcal mol^{-1} at the DFT level. Table 1 summarises the energetics for this case, labelled CPA-MD, and the QM/MM stationary point structures are presented in Fig. 6, with only CEPA and its key interactions within the active site shown for clarity.

Although the (*R*)- and (*S*)-forms take up different binding conformations, in each case: the phenyl group remains bound in the S_1' pocket; the carboxylate maintains its hydrogen bonds to Arg-145; and the chloro-group is bound to the Zn cofactor, although considerably more loosely in the (*S*)-form (3.4 Å) than for the (*R*)-form (2.2 Å). Furthermore, in the (*S*)-form Glu-270 has a quite different orientation, and is not aligned for an S_N2 reaction as it is in the (*R*)-form. In both (*R*)- and (*S*)-transition states, the carboxylate of Glu-270 is oriented to stabilise the aziridinium moiety and is aligned for subsequent reaction. In both the transition states the chloride is strongly bound to the Zn ion at 2.2 Å, and effectively dissociated from the ethylamino chain so that reaction appears to be more S_N1 than S_N2 in character; this is not unsurprising given the hindered orientation of the chloro-leaving group with respect to the amino-nucleophile. This contrasts with the gas phase models which showed S_N2 character where unhindered conformations were used with the fully DFT approach. We should also note that the QM/MM TS structures, although reflecting aziridinium intermediate formation, do not rule out the alternative pathway (Fig. 3(c)) with Glu-270 as a direct nucleophile, since Glu-270 is partially restrained by the link atom in the transition states found here.

7. Conclusions

We have investigated the binding of the two enantiomers of a model (CEPA) of the novel inhibitor, CEMPA, proposed by Park et al. [7] In their original paper, the relative rate of the (*S*)-enantiomeric form of CEMPA was found to inactivate CPA at a slower rate than the (*R*)-enantiomer: It was postulated that this difference was due to different binding motifs allowing the Zn(II) ion of CPA to stabilise the reaction for formation of the aziridinium intermediate with the (*R*)-form; a pathway which was thought to be inaccessible to the (*S*)-form due to binding where the chloro-group did not coordinate with the Zn(II) ion. However, in energetic terms, we note that that the difference in the barriers between the two forms, arising from the observed kinetic rate constants, would be very small. Our quantum mechanical calculations suggest that the reaction barrier for

the (*S*)-form would be considerably larger than the (*R*)-form should stabilisation by Zn(II) not be possible.

Using basic QM/MM methods, we have investigated several possible enzyme configurations with the two enantiomers of CEPA bound, and have shown that both (*R*)- and (*S*)-forms can bind to CPA with the chloro-group within the coordination shell of Zn. When bound in these conformations we would anticipate that their reaction barriers could be very similar; however, it is clear that a reaction for both isomers is quite constrained by the enzyme environment, particularly for the (*S*)-form, and therefore the activation barriers for the inactivation reaction are particularly sensitive to the protein conformation. We have shown that despite the different stresses upon the two isomeric forms, it appears possible that the active site of CPA is sufficiently flexible to accommodate both forms such that Zn can stabilise the inactivation process. Although the methodology used in this work did not result in optimal relaxation of the protein structure, we have found docked conformations which give approximate activation barriers of similar magnitude at the QM/MM level, in agreement with experimental observations. Binding either form of CEPA into a single enzyme configuration based upon (crystal) structures with a natural substrate did not explain the experimental results and thus highlights the importance of active site flexibility in binding these reactive inhibitors.

Future work in this area will consider QM/MM models utilising higher level quantum methods and which incorporate greater MM flexibility, or ideally proper configuration sampling of the enzyme structure to obtain properly averaged free energy barriers.

Acknowledgements

We would like to thank the EPSRC and the University of Manchester for DTA support for this research. We also acknowledge DTI project QCBB/013/00021C for support.

References

[1] A. Fersht, Structure and Mechanism in Protein Science: A Guide to Enzyme Catalysis and Protein Folding, Freeman & Co., 1998.
[2] W.L. Mock, in: M. Sinnott (Ed.), Comprehensive Biological Catalysis, vol. 1, Academic Press, 1998, p. 425.
[3] J. Suh, S.H. Lee, J.Y. Uh, Zn(II)-chelating inhibitors of carboxypeptidase A, Bioorg. Med. Chem. Lett. 5 (1995) 585–588.
[4] X. Hu, W.H. Shelver, Docking studies of matrix metalloproteinase inhibitors: zinc parameter optimisation to improve the binding free energy prediction, J. Mol. Graphics Modell. 22 (2003) 115–126.
[5] G. Liang, J.F. Sebastian, Searching for the lowest energy conformation of substrates in the carboxypeptidase A active site using monte carlo/energy minimisation techniques, Bioinorg. Chem. 26 (1998) 295–308.
[6] L. Banci, I. Bertini, G. La Penna, The enzymatic mechanism of carboxypeptidase: a molecular dynamics study, Proteins 18 (1994) 186–197.
[7] J.D. Park, K.J. Lee, D.H. Kim, A new inhibitor design strategy for carboxypeptidase A as exemplified by *N*-(2-Chloroethyl)-*N*-methylphenylalanine, Biorg. Med. Chem. 9 (2001) 237–243.
[8] S. Alvarez-Santos, A. Gonzalez-Lafont, J.M. Lluch, B. Oliva, F.X. Aviles, On the water-promoted mechanism of peptide cleavage by carboxypeptidase A. A theoretical study, Can. J. Chem. 72 (1994) 2077–2083.
[9] S. Alvarez-Santos, A. Gonzalez-Lafont, J.M. Lluch, B. Oliva, F.X. Aviles, Theoretical study of the role of arginine 127 in the water-promoted mechanism of peptide cleavage by carboxypeptidase A, New J. Chem. 22 (1998) 319–325.
[10] J.H. Cho, D.H. Kim, J.J. Lee, K.Y. Choi, The role of Tyr248 probed by mutant bovine carboxypeptidase A: insight into the catalytic mechanism of carboxypeptidase A, Biochemistry 40 (2001) 10197–10203.
[11] A. Kilshtain-Vardi, G. Shoham, A. Goldblum, Mechanism of action of zinc proteinases: a MNDO/d/H study of the alternative general-acid general-base catalytic pathways for carboxypeptidase-A, Int. J. Quantum Chem. 88 (2002) 87–98.
[12] D.W. Christianson, W.N. Lipscomb, X-ray crystallographic investigation of substrate binding to carboxypeptidase A at subzero temperature, Proc. Nat. Acad. Sci. 83 (1986) 7568.
[13] W.L. Mock, J.Z. Zhang, Mechanistically significant diastereoselection in the sulfoximine inhibition of carboxypeptidase A, J. Biol. Chem. 266 (1991) 6393–6400.
[14] S.-E. Ryu, H.-J. Choi, D.H. Kim, Stereochemistry in inactivation of carboxypeptidase A: structural analysis of the inactivated carboxypeptidase A by an enantiomeric pair of 2-benzyl-3,4-epoxybutanoic acids, J. Am. Chem. Soc. 119 (1997) 38–41.
[15] R.J. Hall, S.A. Hindle, N.A. Burton, I.H. Hillier, Aspects of hybrid QM/MM calculations: the treatment of the QM/MM interface region with an application to chorismate mutase, J. Comput. Chem. 21 (2000) 1433–1441.
[16] M.J. Harrison, N.A. Burton, I.H. Hillier, Catalytic mechanism of the enzyme papain: predictions with a hybrid quantum mechanical/molecular mechanical potential, J. Am. Chem. Soc. 119 (1997) 12285–12291.
[17] A. Warshel, Computer simulations of enzyme catalysis: methods, progress and insights, Annu. Rev. Biophys. Biomol. Struct. 32 (2003) 425–443.
[18] M. Garcia-Viloca, J. Gao, M. Karplus, D.G. Truhlar, How enzymes work: analysis by modern rate theory and computational simulations, Science 303 (2004) 186–195.
[19] M.J. Frisch, G.W. Trucks, H.B. Schlegel, P.M.W. Gill, B.G. Johnson, M.A. Robb, J.R. Cheeseman, T.A. Keith, G.A. Petersson, J.A. Montgomery, K. Raghavachari, M.A. Al-Laham, V.G. Zahrzewski, J.V. Ortiz, J.B. Foresman, J. Cioslowski, B.B. Stefanov, A. Nanayakkara, M. Challacombe, C.Y. Peng, P.Y. Chen, W. Ayala, M.W. Wong, J.L. Andres, E.S. Repogle, R. Gomberts, R.L. Martin, D.J. Fox, J.S. Binkley, D.J. Defrees, J. Baker, J.P. Stewart, M. Head-Gordon, C. Gonzales, J.A. Pople, Gaussian 94, Gaussian Inc., Pittsburgh, 1994.
[20] W.D. Cornell, P. Cieplak, C.I. Bayly, I.R. Gould, K.M. Merz, D.M. Ferguson, D.C. Spellmeyer, T. Fox, J.W. Caldwell, P.A. Kollman, J. Am. Chem. Soc. 117 (1995) 5179.
[21] M.P. Gleeson, I.H. Hillier, N.A. Burton, Theoretical analysis of peptidyl α-ketoheterocyclic inhibitors of human neutrophil elastase: insight into the mechanism of inhibition and the application of QM/MM calculations in structure-based drug design, Org. Biomol. Chem. 2 (2004) 2275–2280.
[22] D.A. Pearlman, D.A. Case, J.W. Caldwell, W.S. Ross, T.E. Cheatham, D.M. Ferguson, G.L. Seibel, U.C. Singh, P.K. Weiner and P.A. Kollman, AMBER 4.1, University of California, San Francisco, 1995.
[23] G.M. Morris, D.S. Goodsell, R.S. Halliday, R. Huey, W.E. Hart, R.K. Belew, A.J. Olson, Automated docking using a lamarckian genetic algorithm and empirical binding free energy function, J. Comput. Chem. 19 (1998) 1639–1662.